Neuron
Article

Satb2 Regulates Callosal Projection Neuron Identity in the Developing Cerebral Cortex

Elizabeth A. Alcamo,[1,4,5] Laura Chirivella,[2,4] Marcel Dautzenberg,[3] Gergana Dobreva,[3] Isabel Fariñas,[2] Rudolf Grosschedl,[3,*] and Susan K. McConnell[1,*]
[1]Department of Biology, Stanford University, Stanford, CA 94305, USA
[2]Departamento de Biología Celular and Unidad Mixta CIPF-UVEG, Universidad de Valencia, 46100 Burjassot, Spain
[3]Max-Planck Institute of Immunobiology, 79108 Freiburg, Germany
[4]These authors contributed equally to this work.
[5]Present address: Department of Ophthalmics Research, Merck & Co., Inc., West Point, PA 19486, USA.
*Correspondence: grosschedl@immunbio.mpg.de (R.G.), suemcc@stanford.edu (S.K.M.)
DOI 10.1016/j.neuron.2007.12.012

SUMMARY

Satb2 is a DNA-binding protein that regulates chromatin organization and gene expression. In the developing brain, *Satb2* is expressed in cortical neurons that extend axons across the corpus callosum. To assess the role of Satb2 in neurons, we analyzed mice in which the *Satb2* locus was disrupted by insertion of a *LacZ* gene. In mutant mice, β-galactosidase-labeled axons are absent from the corpus callosum and instead descend along the corticospinal tract. *Satb2* mutant neurons acquire expression of Ctip2, a transcription factor that is necessary and sufficient for the extension of subcortical projections by cortical neurons. Conversely, ectopic expression of Satb2 in neural stem cells markedly decreases Ctip2 expression. Finally, we find that Satb2 binds directly to regulatory regions of *Ctip2* and induces changes in chromatin structure. These data suggest that Satb2 functions as a repressor of *Ctip2* and regulatory determinant of corticocortical connections in the developing cerebral cortex.

INTRODUCTION

Projection neurons in the mammalian cerebral cortex comprise two broad classes: those that extend axons within the cortex, including those that cross the corpus callosum to the contralateral hemisphere; and those that form connections with subcortical targets, including the thalamus, midbrain, hindbrain, and spinal cord (McConnell, 1995; Molyneaux et al., 2007). While the latter neurons are located primarily in cortical layers 5 and 6, neurons with cortical and callosal projections are found in all layers but are particularly abundant in layers 2 through 4. During development, neurons in different layers are generated in an orderly inside-first, outside-last procession, and newly postmitotic neurons are specified to adopt the laminar positions characteristic of their birthdays (McConnell, 1995). Neurons with different projection phenotypes can be generated at the same time. For example, layer 5 neurons that form callosal versus subcortical projections migrate and differentiate side-by-side, but their axon trajectories diverge immediately, extending toward the midline and internal capsule, respectively (Koester and O'Leary, 1993, 1994).

Two genes required for the development of layer 5 subcortical projection neurons are *Fezf2* and *Ctip2*, which encode zinc-finger transcription factors. Both are expressed by developing layer 5 and 6 neurons and show prominent expression in corticospinal motor neurons (CSMNs). In *Fezf2* mutant mice, deep-layer neurons are generated and migrate into appropriate positions but fail to express *Ctip2* (Chen et al., 2005a; Molyneaux et al., 2005). Deletion of either *Fezf2* or *Ctip2* disrupts formation of the corticospinal tract (Arlotta et al., 2005; Chen et al., 2005a, 2005b; Molyneaux et al., 2005), and ectopic expression of *Fezf2* or *Ctip2* in layer 2/3 neurons, which normally form corticocortical connections, is sufficient to direct their axons subcortically (Chen et al., 2005b; Molyneaux et al., 2005; B. Chen and S.K.M., unpublished data). These data suggest that Fezf2 and Ctip2 function in a common pathway that is necessary and sufficient for the specification of subcortical projection neurons in cortical layer 5.

Despite the progress above, little is understood about how corticocortical (ipsilateral and callosal) projection neurons are specified. One potential regulatory determinant of this cell type is the DNA-binding protein Satb2, which is expressed in a subset of neurons in layers 2 through 5 during differentiation (Britanova et al., 2005; Dobreva et al., 2006; Szemes et al., 2006). Satb transcription factors regulate gene expression by binding AT-rich sequences of matrix attachment regions (MARs), promoting higher-order chromatin organization and facilitating long-range interactions between enhancers and promoters (Jenuwein et al., 1997; Cai et al., 2003; Dobreva et al., 2003; Britanova et al., 2005). Satb2 functions in B cell differentiation by binding to MAR sequences in and augmenting expression of the immunoglobulin μ heavy chain locus (Dobreva et al., 2003). Satb2 also regulates osteoblast differentiation and function by repressing *Hoxa2* and activating osteoblast-specific gene expression via enhancement of two key determinants of osteoblast differentiation, *Runx2* and *ATF4* (Dobreva et al., 2006).

To assess the role of Satb2 in cortical development, we analyzed Satb2-deficient mice in which the bacterial β-galactosidase (*LacZ*) gene was inserted in-frame with the first ATG codon

of *Satb2* (Dobreva et al., 2006). We find that the axons of *Satb2*-expressing cortical neurons in heterozygous mice are labeled by β-galactosidase and extend across the corpus callosum. In *Satb2* mutants, β-galactosidase$^+$ axons are absent from the corpus callosum and instead descend through the internal capsule and along the corticospinal tract, suggesting that *Satb2*-deficient callosal neurons adopt a subcortical projection neuron fate. *Satb2* mutant neurons acquire expression of *Ctip2*, which is necessary and sufficient for the elaboration of subcortical axon projections (Arlotta et al., 2005; B. Chen and S.K.M., unpublished data). Our data show that Satb2 binds directly to regulatory regions of *Ctip2* and represses *Ctip2* expression, suggesting that Satb2 functions in normal cortical development to repress *Ctip2* and enable the formation of corticocortical connections.

RESULTS

Cortical Neurons that Express *Satb2* Extend Axons across the Corpus Callosum

Within the telencephalon, Satb2-expressing cells are restricted to the developing cerebral cortex. Consistent with previous reports (Britanova et al., 2005; Szemes et al., 2006), Satb2-immunoreactive cells were first detected in lateral regions of the cortical plate (CP) at E13.5 (see Figure S1A available online). Both the number of Satb2$^+$ cells and the intensity of staining increased over time, with many immunoreactive cells observed in the CP by E18.5 (Figures S1B–S1E). The number of Satb2$^+$ cells was dramatically reduced by P7 (Figure S1F), when cortical neurons have finished migrating and are refining their axonal projections.

To further characterize the subpopulation of Satb2$^+$ cells, E18.5 brains were immunostained for Satb2 and a panel of layer-specific markers. Most Satb2$^+$ cells resided in layers 2 through 4 of the CP, a domain that also expressed the homeodomain protein Cux2 (Figure 1A). The majority of Cux2$^+$ cells coexpressed Satb2, although many Satb2$^+$ cells (particularly those in deeper layers) were Cux2$^-$. A smaller number of Satb2$^+$ cells were present in layer 5 and even fewer in layer 6, layers that are defined by an immunoreactivity for Ctip2 and Tbr1, respectively (Figures 1B and 1C). Little coexpression was observed between Satb2 and these deep-layer markers, with <5% of Satb2$^+$ cells expressing Ctip2 (Figure 1B). Colocalization of Satb2 and the neuron-specific marker MAP2 demonstrated that Satb2$^+$ cortical cells are postmitotic neurons (Figure 1E, insert). No Satb2$^+$ cells were detected in zones of active proliferation, including the Tbr2$^+$ subventricular zone (SVZ; Figure 1D) and the subjacent ventricular zone (VZ). Weak Satb2 immunoreactivity was detected in the intermediate zone (IZ) (Figure 1). These data suggest that Satb2 is not expressed by cortical neurons prior to migration.

Satb2-expressing neurons can be detected in *Satb2*$^{+/lacZ}$ mice (Dobreva et al., 2006) by the presence of β-galactosidase, which is strongly expressed in the CP at E18.5. Immunostaining for Satb2 and β-galactosidase revealed that these proteins are present in the nucleus and cytoplasm, respectively, of the same cells, confirming that *LacZ* expression recapitulates that of *Satb2* (Figure 1E). β-galactosidase immunoreactivity was most prominent in the superficial CP (layer 2/3), in which most cell bodies were labeled, and less prominent in the deep layers, similar to Satb2 staining. In addition, it appeared that β-galactosidase was transported into axons, since the IZ (deep band in Figure 1E), where cortical efferent axons are located, was also labeled.

The transport of β-galactosidase into axons in *Satb2*$^{+/lacZ}$ mice enabled us to trace the projections of *Satb2*-expressing neurons. Both X-gal staining and immunohistochemistry at E18.5 revealed β-galactosidase$^+$ axons crossing the corpus callosum (Figure 3E and Figure S2). No labeling was observed in the internal or external capsules (Figures 3E–3H), where axons exit the cortex toward subcortical targets, suggesting that Satb2$^+$ neurons form callosal connections. A few labeled axons were visible in the striatum (Figure S2), where some callosal projection neurons form axon collaterals (Wilson, 1987). Most of the labeled callosal axons were likely derived from deep-layer Satb2$^+$ neurons, since layer 5 cells are the earliest in the CP to extend callosal axons (Ozaki and Wahlsten, 1998). However, some labeled axons may belong to migrating layer 2/3 neurons, which extend axons to the contralateral cortex by E19 in mouse (Auladell et al., 1995). Collectively, these data suggest that *Satb2*-expressing cortical neurons extend axons to the contralateral cortex. We do not know whether Satb2$^+$ neurons also form ipsilateral corticocortical projections, but this is likely in light of previous findings that many callosal neurons also form local axon branches (Veinante and Deschenes, 2003; Mitchell and Macklis, 2005; Petreanu et al., 2007).

Defects in Migration in *Satb2* Mutant Mice

Because *Satb2* null mice die at birth (Dobreva et al., 2006), tissue was collected from wild-type, *Satb2*$^{+/-}$, and *Satb2*$^{-/-}$ embryos at E18.5. Cresyl violet staining revealed that the *Satb2*-deficient cortex was organized normally, with a clearly defined VZ, SVZ, IZ, and CP (Figures 2A and 2B). However, mutants exhibited small but significant reductions in cortical thickness at E18.5, with decreases of ~15% in CP thickness and up to 20% in the width of the IZ (Figure S3). Cell density in the CP and IZ did not differ significantly between genotypes (*Satb2*$^{+/+}$ CP, 11,500 ± 500 cells/mm^2; IZ, 11,500 ± 500 cells/mm^2; n = 3. *Satb2*$^{-/-}$ CP, 11,500 ± 645; IZ, 11,750 ± 946 cells/mm^2; n = 4). These data suggest that the mutant cortices had an overall reduction of ~15% in the total number of cells compared to wild-type controls. Although the lateral ventricles of *Satb2* mutants were somewhat enlarged (cf. Figure 3), we saw no significant difference in the thickness of the proliferative zones (Figure S3).

The decreased thickness of the CP could result from altered proliferation, survival, and/or migration. A direct role of Satb2 in cell proliferation seems unlikely, since *Satb2* is not obviously expressed in cortical proliferative zones (Britanova et al., 2005; Szemes et al., 2006) (see Figure 1). Furthermore, we observed no differences in the number of pyknotic nuclei between wild-type and mutants (data not shown), suggesting that the thinner CP is not due to increased cell death. To assess migration, proliferating cells were labeled with BrdU at E11.5, E13.5, or E15.5, and positions of labeled progeny were assessed on E18.5. Because the mutant cortex was slightly thinner than in controls, we divided the dorsal CP into upper, middle, and lower thirds (Figures 2C and 2D) and counted BrdU$^+$ cells within

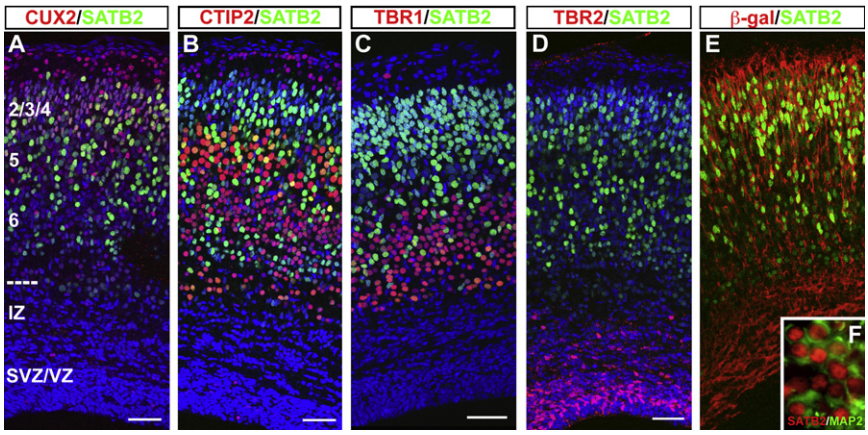

Figure 1. Satb2 Is Expressed by a Subset of Neurons in Cortical Layers 2 through 5

Each panel shows the immunohistochemical localization of proteins in the E18.5 wild-type cortex.

(A) Cux2 (red) is expressed primarily in layer 2/3 neurons, where it shows substantial coexpression with Satb2 (green).

(B) Ctip2 (red) and Satb2 (green) are expressed in largely nonoverlapping populations of cortical cells. Layer 5 cells express high levels of Ctip2, and lower levels are apparent in layer 6, whereas Satb2 predominates in more superficial layers.

(C) Satb2 (green) and the layer 6-specific marker Tbr1 (red) are expressed in spatially segregated domains in the developing cortex.

(D) Satb2 (green) is not expressed by cells of the SVZ, marked by Tbr2 (red).

(E) Immunohistochemistry for β-galactosidase (red) and Satb2 (green) in *Satb2*$^{+/lacZ}$ embryos demonstrates that β-galactosidase is expressed by *Satb2*$^{+}$ neurons. Note that β-galactosidase is detected in both cell bodies within the cortical plate (CP) and axons in the intermediate zone (IZ).

(F) High-magnification image revealing colocalization of nuclear Satb2 (red) with cytoplasmic staining for the neuron-specific marker MAP2 (green), demonstrating that Satb2 is expressed in postmitotic neurons. Scale bar, 50 μm.

each subdomain and in the IZ and VZ/SVZ. As expected, since few neurons express *Satb2* at E11.5 (Britanova et al., 2005), no differences were observed at E11.5; in both mutant versus wild-type brains, most BrdU^{+} cells were in the deep CP (Figure 2E). In contrast, cells labeled at E13.5 migrated differently in wild-type versus *Satb2*$^{-/-}$ embryos, with significantly fewer BrdU^{+} cells in the upper CP of *Satb2*$^{-/-}$ brains and a commensurate increase in cells occupying the IZ (Figure 2E). Cells born at E15.5 also showed defective migration, with a significant reduction in BrdU^{+} cells in the upper and middle CP and an increased fraction in the IZ of mutants at E18.5 (Figure 2E). Sections stained for both BrdU and β-galactosidase following E15.5 BrdU injections revealed that not all BrdU^{+} cells in the IZ were β-galactosidase^{+} (Figure 2F), suggesting that at least some defects in migration reflect a cell-nonautonomous role for Satb2.

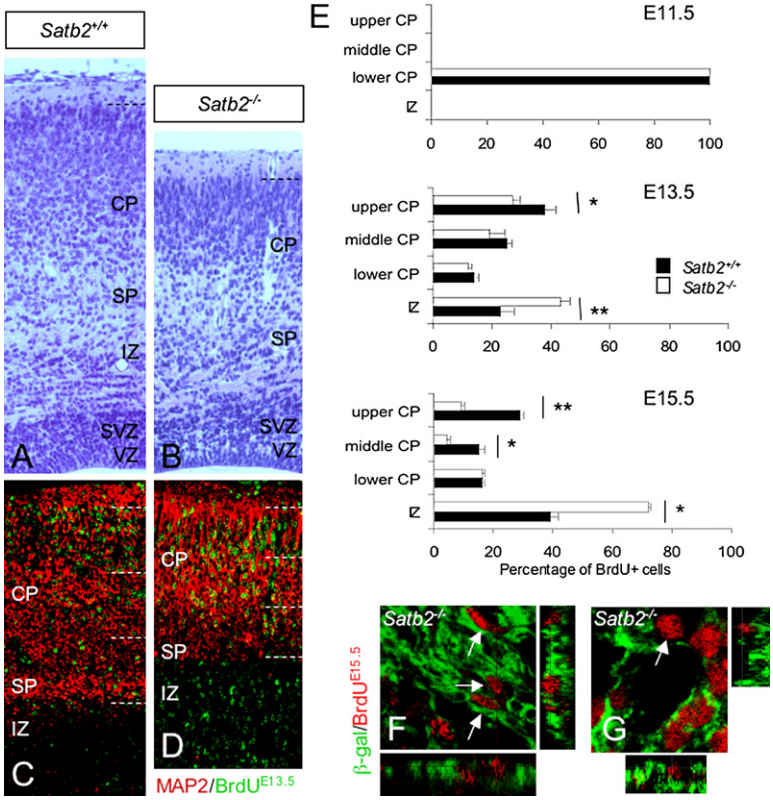

Figure 2. Defects in Migration in the *Satb2*-Deficient Cortex

(A and B) Cresyl violet staining of sections through the E18.5 *Satb2*$^{+/+}$ and *Satb2*$^{-/-}$ cortex, showing that the cerebral wall in *Satb2*$^{-/-}$ mutants is smaller than that in wild-type mice.

(C and D) Immunohistochemistry for BrdU and MAP2 in E18.5 cortices of *Satb2*$^{+/+}$ and *Satb2*$^{-/-}$ embryos injected with BrdU at E13.5 (E13.5^{BrdU}), showing that a fraction of *Satb2*-deficient neurons born at E13.5 do not migrate appropriately. The dashed lines show the demarcation of the cortical plate into upper, middle, and lower thirds.

(E) Quantitation of BrdU^{+} cells in the cortical plate of E18.5 *SatB2*$^{+/+}$ (black bars) and *SatB2*$^{-/-}$ (white bars) embryos injected with a single injection of BrdU at E11.5, E13.5, or E15.5. The positions of BrdU^{+} cells in the VZ/SVZ, intermediate zone (IZ), and the upper, middle, and lower regions of the cortical plate (CP) were quantitated from brain sections. The counts are represented as the percentage of BrdU^{+} cells in each region relative to the total number of cells labeled by the injection. Statistically significant differences were found at E13.5 and E15.5 (*$p < 0.05$, **$p < 0.01$; Student's t test). BrdU^{+} cells marked at E13.5 and E15.5 failed to migrate properly and accumulated in the IZ. Error bars show mean ± SD.

(F and G) Confocal microscopic images of cells pulse-labeled with BrdU at E15.5 (red, BrdU$^{E15.5}$) found in the intermediate zone of *Satb2* mutants at E18.5. Some BrdU^{+} cells also expressed β-galactosidase immunoreactivity (arrows in [F]), whereas others did not (arrow in [G]). The panels adjacent to (F) and (G) correspond to the x-z (bottom) and y-z (right) planes of three-dimensional reconstructions.

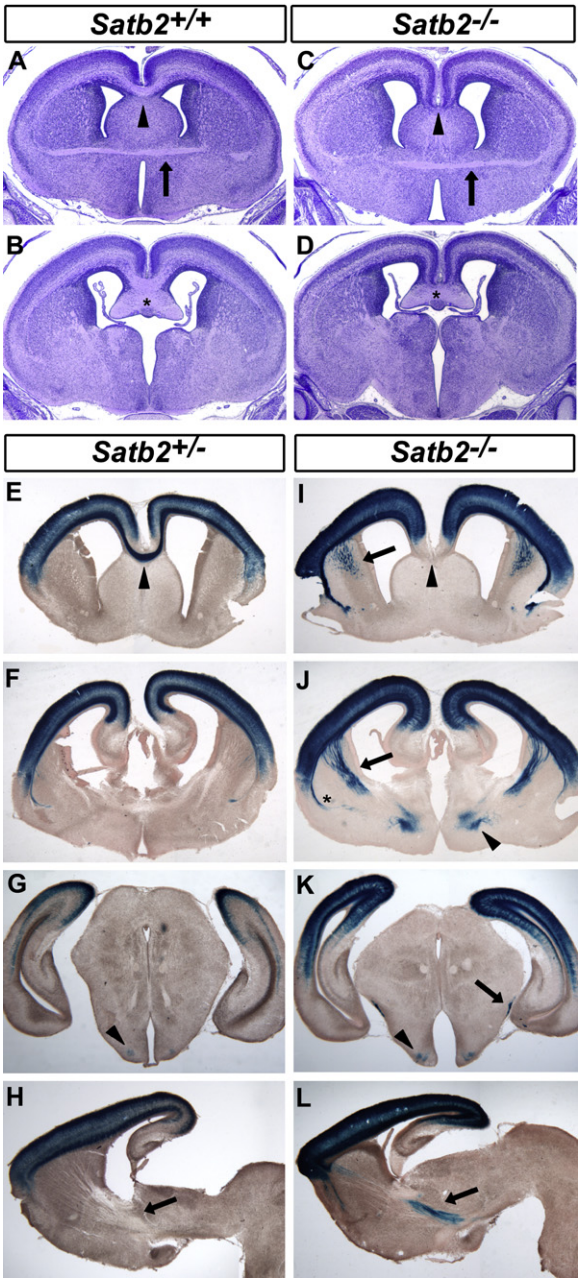

Figure 3. *Satb2*-Expressing Neurons that Normally Project across the Corpus Callosum Extend Axons into Subcortical Regions in the Absence of Satb2

(A–D) Coronal sections through the brains of wild-type and *Satb2* null embryos at E18.5.

(A and B) Wild-type brain, highlighting the normal positions of the corpus callosum (arrowheads) and anterior (arrows) and hippocampal (asterisks) commissures.

(C and D) Cresyl violet staining of *Satb2* mutant brains reveals a severely reduced corpus callosum (arrowhead), whereas the anterior (arrow) and hippocampal (asterisk) commissures are intact. Mutant brains have an apparently normal cytoarchitecture, although cortical thickness is slightly reduced and the lateral ventricles are enlarged.

(E–L) X-gal histochemistry for β-galactosidase on coronal and sagittal sections of E18.5 *Satb2*$^{+/-}$ and *Satb2*$^{-/-}$ brains at equivalent planes of section shows changes in the projection patterns of β-galactoside^{+} axons in mutants. In heterozygotes (E–H), β-galactoside^{+} axons project across the corpus callosum, whereas in *Satb2* knockouts (I–L), β-galactoside^{+} axons project into the internal and external capsules ([J], arrows and asterisks, respectively). Arrow in (K) denotes the most caudal visualization of β-galactoside-labeled axons in the cerebral peduncle. Arrowheads in (J) denote labeling in mutants of an unidentified ventromedial structure. Weak labeling was observed in this region in *Satb2*$^{+/-}$ brains; thus it is possible that this label is from hypothalamic nuclei that are labeled more intensely in *Satb2*$^{-/-}$ due to the presence of two *LacZ* alleles. Alternatively, this may represent labeling of the medial forebrain bundle due to as yet uncharacterized aberrant projections. Arrowheads in (G) and (K) denote ventral mammary nuclei that are labeled in both *Satb2*$^{+/-}$ and *Satb2*$^{-/-}$ brains.

The Axons of *Satb2*-Deficient Neurons Fail to Cross the Corpus Callosum and Instead Project Subcortically

In addition to a modest reduction in cortical thickness, *Satb2* mutants displayed striking alterations in axonal connectivity. Cresyl violet-stained coronal sections from E18.5 embryos revealed the apparent absence of the corpus callosum in *Satb2* mutants (Figures 3A–3D). Other major forebrain axon tracts such as the anterior and hippocampal commissures (Figures 3C and 3D) appeared normal, suggesting that there were not global defects in midline development. The width of the corpus callosum was similar in *Satb2*$^{+/-}$ and wild-type brains (wild-type, 128 ± 17 μm; *Satb2*$^{+/-}$, 138 ± 9 μm; n = 3), suggesting that callosal connectivity is normal in heterozygotes.

To ascertain whether the axons of *Satb2*-deficient neurons extended across the corpus callosum, β-galactosidase activity was visualized using X-gal histochemistry (Figures 3E–3L) and immunohistochemistry (Figure S2). Although β-galactosidase^{+} cell bodies were observed in the CP, neither method stained callosal axons in *Satb2* mutants (Figure 3I and Figure S2), suggesting that neurons that normally express *Satb2* are generated and migrate into the CP but do not project axons to their normal contralateral targets.

Failures of callosal development are common in mutant mice (Richards et al., 2004) and are often accompanied by the formation of Probst bundles, in which callosal axons accumulate on either side of the midline (Stefanko, 1980; Ozaki and Wahlsten, 1993). In *Satb2*-deficient mice, however, Probst bundles were not observed using Cresyl violet staining (Figures 3C and 3D), X-gal histochemistry (Figure 3I), or β-galactosidase immunoreactivity (Figure S2), suggesting that *Satb2*-deficient axons assumed a novel trajectory rather than approaching the callosum and stalling. To visualize these axons, we serially sectioned *Satb*$^{+/-}$ and mutant brains, then used X-gal histochemistry (Figures 3I–3L) and immunohistochemistry (Figure S2) to reveal β-galactosidase. These experiments revealed large numbers of β-galactosidase^{+} axons in the internal capsule in *Satb2*$^{-/-}$ mice (Figures 3I, 3J, and 3L and Figure S2). Labeled axons projected along the path normally traversed by corticospinal axons, descending caudoventrally in the cerebral peduncle and pyramidal tract to roughly the level of the substantia nigra (Figures 3I–3L and Figure S2). We also observed an increased number of β-galactosidase^{+} axons in the striatum of *Satb2* mutants (Figure 3I and Figure S2). In normal animals, many layer 5 subcortical projection neurons form collaterals in the striatum (Reiner et al., 2003), thus we hypothesize that labeled axons in the striatum are collaterals from subcortically projecting axons.

β-galactosidase$^+$ axons in *Satb2* mutants were also seen in the external capsule (Figures 3I and 3J and Figure S2), a major conduit to the anterior commissure; however, β-galactosidase$^+$ axons did not enter this commissure (Figure S2). The external capsule also contains axons from dorsal cortical neurons that cross the striatum and the internal capsule (Rouiller and Welker, 1991); thus some β-galactosidase$^+$ axons may join the descending corticospinal tract. It is also possible that these axons innervate the striatum, since axons from deep-layer neurons in sensorimotor cortex can enter striatal targets from the external capsule (Brown et al., 1998).

The Expansion of Subcortical Projections in *Satb2* Mutants Is Not Due to Early Defects in Callosal Development

The studies above suggest that *Satb2*-deficient, β-galactosidase$^+$ neurons alter their normal callosal pattern of axonal projections and instead adopt projections typical of subcortical projection neurons. These altered trajectories could be the consequence of defects in the construction of the callosal pathway itself, disruptions in the expression of axon guidance molecules, or changes in cell-fate specification. We examined each of these possibilities in *Satb2*-deficient mice.

Analysis of the dorsal midline revealed that the corpus callosum is constructed in *Satb2* mutants, but β-galactosidase$^+$ axons do not cross it (Figures 4A–4G). Callosal development requires that a "glial sling" traverse the gap between the two hemispheres before axons can grow contralaterally (Silver et al., 1982; Ashwell and Mai, 1997; Shu et al., 2003). Immunohistochemistry revealed that Satb2 is not expressed at the dorsal midline (Figure 4A) and that GFAP$^+$ glial cells of the induseum griseum and glial wedge (Figures 4A and 4B) and the NeuN$^+$ glial sling (Figure 4B) are present and appear normal in *Satb2* mutants (Figure 4E). Staining for the neural cell adhesion molecules L1, which labels most growing axons (Fujimori et al., 2000; Mintz et al., 2003), and TAG-1, which marks commissural neurons (Wolfer et al., 1994; Fujimori et al., 2000), revealed that a small population of β-galactosidase-negative axons do cross the corpus callosum in *Satb2* mutants (Figures 4F and 4G). Thus, the callosal structure across which Satb2$^+$ axons would normally cross is intact in *Satb2* mutants.

We then analyzed the expression of molecules that are normally expressed at the dorsal midline and regulate axon guidance (reviewed in Lindwall et al., 2007). In situ hybridization of control and *Satb2* null brains at E14.5 and E18.5 for 32 axon guidance ligands, including members of the *Netrin*, *Slit*, *Semaphorin*, *Ephrin-A* and *Ephrin-B* gene families (Table S1), revealed no obvious changes in expression at the telencephalic midline (data not shown). These results, in conjunction with evidence that the corpus callosum does form in *Satb2* mutants, suggest that *Satb2* mutants show cell-autonomous changes in axon targeting rather than defects that preclude callosal axons from crossing the midline.

Alterations in Layer Identity in the *Satb2*-Deficient Cortex

To examine potential changes in the fates of *Satb2*$^{-/-}$ neurons, we assessed the expression of layer-specific markers for subcortical projection neurons. *Satb2* mutants showed normal expression of Tbr1 (Figures 5A and 5B), which regulates the formation of corticothalamic projections from layer 6 (Hevner et al., 2001, 2002). In contrast, we observed a marked expansion in the expression of Ctip2 (Figures 5G–5J), which is normally expressed at high levels in layer 5 and regulates subcortical projection neuron identity (Arlotta et al., 2005; B. Chen and S.K.M., unpublished data). In *Satb2* mutants, Ctip2 expression expanded to encompass the superficial CP (Figures 5H and 5J), which normally contains layer 2/3 corticocortical projection neurons. The number of Ctip2$^+$ cells in layer 5 also increased, as expected if layer 5 callosal projection neurons (which normally lack Ctip2: Arlotta et al., 2005) acquired a CSMN identity (Figures 5H and 5J). Immunostaining with antibodies against both Ctip2 and β-galactosidase revealed that neurons throughout the CP of *Satb2* mutants coexpressed both markers (Figure 5H), indicating that neurons that normally express *Satb2* acquired the expression of Ctip2 in mutants.

To confirm that Ctip2 is expressed ectopically in neurons normally destined to become layer 2/3 corticocortical neurons, progenitors were labeled with BrdU on E15.5 (when layer 2/3 neurons are generated) and brains were collected at E18.5, after neurons have migrated into the CP. In controls, BrdU$^+$ cells in the CP were Ctip2$^-$ (Figures 5I and 5M); in contrast, BrdU$^+$ cells in the CP of *Satb2* mutants expressed Ctip2 (Figures 5J–5L and 5N–5P). These experiments show definitively that upper-layer neurons acquired Ctip2 expression in the absence of *Satb2*. Similarly, when embryos were pulsed with BrdU at E13.5 to mark layer 5 and examined at E18.5, a greater fraction of BrdU$^+$ cortical cells were Ctip2$^+$ in *Satb2* mutants compared to controls (data not shown). Collectively, these results demonstrate that the Ctip2$^+$ cell population in the cortex expands in *Satb2*-deficient animals to include cells that normally differentiate into layer 2/3 corticocortical neurons and layer 5 cells normally destined to become non-CSMN subtypes.

Normal animals show little or no overlap in the cortical expression domains of Ctip2 and Cux2, with Ctip2$^+$ cells in deep layers and Cux2$^+$ cells located superficially (cf. Figures 1A and 1B and Figures 5C, 5G, and 5I). Although *Satb2*-deficient, β-galactosidase$^+$ cells destined for the superficial CP in *Satb2* mutants acquired Ctip2 expression and extended subcortical axons, both characteristics of layer 5 CSMNs, significant Cux2 expression was still observed in the superficial CP (Figure 5D). Additionally, many Cux2$^+$ cells adopted abnormal positions in the mutant brain, in the deep CP or IZ (Figure 5D), consistent with disruptions in cell migration (cf. Figure 2E). These observations suggest that *Satb2*-deficient neurons may express combinations of transcription factors (e.g., Ctip2 and Cux2) that are normally not coexpressed, generating conflicting signals within cells that may disrupt migration.

Altered Expression of Genes Associated with Subcortical and Callosal Projection Phenotypes in the *Satb2* Mutant Cortex

The studies above suggest that callosal projection neurons normally express *Satb2*, that these cells adopt many aspects of a subcortical projection neuron identity in the absence of *Satb2*, and that Satb2 antagonizes expression of *Ctip2*, a gene

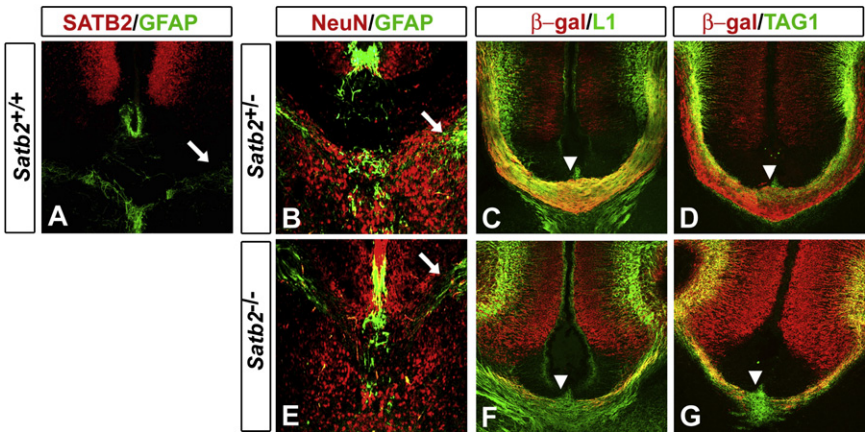

Figure 4. The Establishment of the Corpus Callosum Appears Normal in *Satb2* Mutant Brains

(A) Satb2 (red) is not expressed at the dorsal midline where the corpus callosum forms, or by cells of the glial wedge ($GFAP^+$ cells, green, denoted by arrow).

(B and E) Immunohistochemistry for the glial sling marker NeuN (red) and the glial wedge marker GFAP (green) shows that the glial sling forms appropriately in *Satb2* mutants.

(C, D, F, and G) Immunofluorescence for β-galactosidase (red) and the axonal markers L1 (C and F) or TAG1 (D and G) demonstrates that a small population of $\beta\text{-gal}^-$ axons still cross the corpus callosum (denoted by arrowhead) in *Satb2* mutants.

important for CSMN development. Previous studies identified several genes expressed selectively by CSMNs or callosal projection neurons (Arlotta et al., 2005). To examine whether Satb2 broadly regulates these transcriptional profiles, we assessed the expression of cell-type- and layer-specific markers by in situ hybridization at E14.5 and E18.5 (Table 1, Figure 6, Table S2, and Figure S4). No differences in expression were observed at E14.5 for any genes assayed (data not shown), but many changes were noted at E18.5.

The expression of several CSMN-specific genes was altered in E18.5 mutants. In addition to *Ctip2*, the cortical expression of the transcriptional coactivator *Clim1/Ldb2*, the cell adhesion molecule *Cdh13*, and the signaling molecule *Grb14* also displayed increased expression levels in layer 5 and an expansion of expression into layer 2/3 (Figures 6A–6D and Table 1). This upregulation of CSMN gene expression supports the notion that *Satb2*-deficient neurons acquired characteristics typical of CSMNs. However, not all CSMN-specific genes showed expanded patterns of expression. For example, the transcription factor *Fezf2*, which is required for CSMN development (Chen et al., 2005b; Molyneaux et al., 2005; B. Chen and S.K.M., unpublished data), was expressed normally in mutants (Figures 6M and 6N and Table S2). These data suggest that *Satb2*-deficient neurons acquire many but not all characteristics of normal CSMNs by E18.5.

To assess the role of *Satb2* in the expression of genes characteristic of callosal neurons, we performed in situ hybridization for the adhesion molecule *Cdh10*, the signaling molecules *Ptn* and *Dkk3*, and the transcriptional corepressor *Lmo4*. In controls, each gene was expressed in the superficial and deep layers of the CP (Figures 6E, 6G, and 6I). All four genes were downregulated in *Satb2* mutants at E18.5 (Figures 6F, 6H, and 6J and Table 1), consistent with a loss of callosal projection neuron identity. In addition, expression of *RORβ* was lost in layer 4 of *Satb2* mutants (Figures 6K and 6L). Since *RORβ* is normally expressed in local projection neurons of layer 4 and a subset of layer 5 neurons (Takeuchi et al., 2006), this suggests a role for *Satb2* in the development of locally projecting corticocortical neurons as well. However, as above, not all patterns of gene expression were altered in a predictable pattern. For example, some transcripts normally present in layer 2/3 expanded their expression to encompass the IZ in mutants (Table 1), although defects in the migration of upper-layer neurons may have contributed to these changes (Figure 2). We observed no obvious change in the expression of Tbr2 by immunohistochemistry (data not shown) or *svet1* by in situ hybridization (Figures 6O and 6P and Table S2), markers for SVZ intermediate progenitor cells that produce layer 2/3 neurons (Tarabykin et al., 2001; Molyneaux et al., 2007).

Acquisition of a CSMN fate at the expense of a callosal one should be accompanied by changes in the expression of guidance molecules that enable axons to pathfind and innervate appropriate targets. Genes that mediate chemoattraction and chemorepulsion, such as *EphA4* (Kullander et al., 2001a, 2001b; Canty et al., 2006), *netrin1* (Barallobre et al., 2000), the Netrin receptors *DCC* and *Unc5h3* (Finger et al., 2002), and *slit1/2* (Bagri et al., 2002), play essential roles in the development of the corpus callosum and corticospinal tract. To identify axonal pathfinding molecules that were misregulated in the *Satb2* mutants and thus might redirect axons to subcortical targets, we assayed the cortical expression of members of the *Eph*, *Ephrin*, *Sema*, *Plexin*, *Robo*, *Slit*, *Netrin*, and *Unc* gene families by in situ hybridization (Table 2, Table S3, and Figure S5). The expression of axon guidance receptors *EphA5*, *EphA7*, *EphB1*, *efnb2*, and *NRP1* was elevated in layer 5 and the superficial CP of *Satb2* mutants, suggesting that they may play roles in pathfinding to subcortical targets. Conversely, expression of the *EphA4*, *PlxnA4*, and *unc5h3* receptor genes was reduced or lost throughout the *Satb2*-deficient CP, suggesting roles in pathfinding either within the cortex or across the corpus callosum. The specific functions of these molecules remain to be tested in future studies.

Satb2 Antagonizes the Expression of Ctip2 by Direct Binding to MAR Sequences in *Ctip2*

The studies above suggest that Satb2 promotes a callosal projection neuron fate by antagonizing the expression of *Ctip2* and other CSMN genes. Studies of wild-type tissue at E18.5 (Figure 1B) support this hypothesis, since <5% of $Ctip2^+$ cells were also $Satb2^+$. To explore the putative antagonism of *Ctip2* by Satb2, we assessed the expression of Satb2 and Ctip2 throughout CP development. From E14.5 onward, <5% of $Ctip2^+$ cells coexpressed Satb2 (Figures 6B, 6B′, 6C, and 6C'). However, at E13.5, ~40% of $Ctip2^+$ cells also expressed Satb2

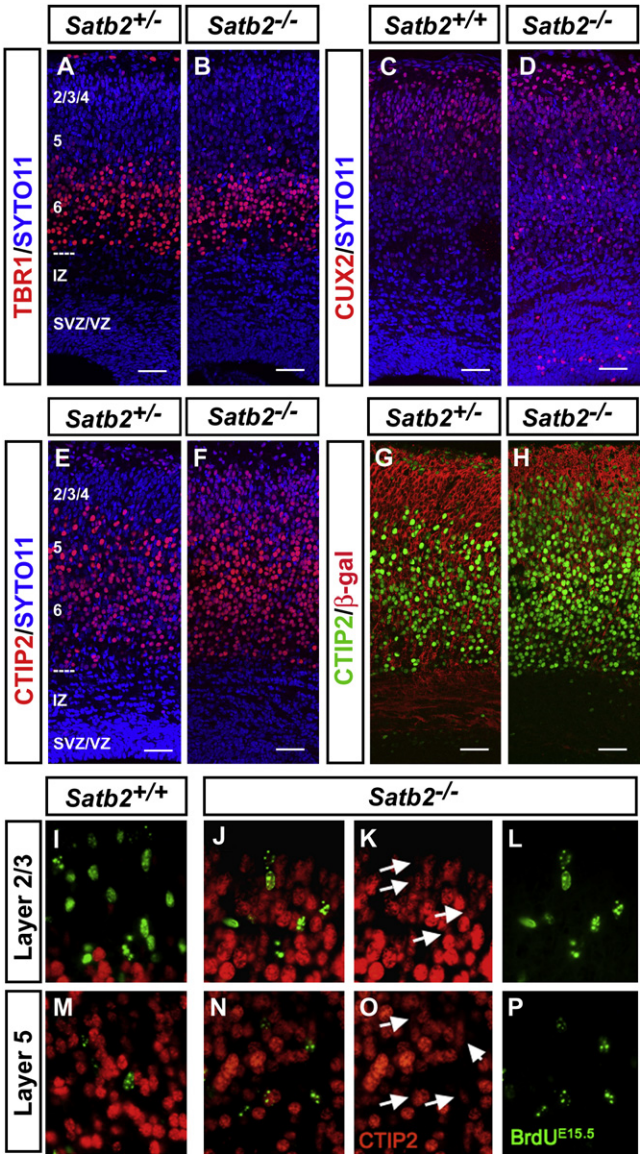

Figure 5. Layer 2/3 Neurons Express the CSMN Gene Ctip2 in *Satb2*-Deficient Mice

(A and B) Tbr1 expression is similar in control and *Satb2*$^{-/-}$ cortex.

(C and D) Immunohistochemistry for Cux2 reveals that the overall size of the Cux2^{+} population appears normal in *Satb2* mutants. However, while many Cux2^{+} neurons reside in the superficial CP in *Satb2* mutants, some Cux2^{+} neurons show migration defects and reside in the deep CP and IZ.

(E and F) Ctip2 immunoreactivity is confined to layers 5 and 6 in the control mouse cortex, but has expanded in both cell number and domain in the absence of *Satb2* to include cells in the superficial CP as well as additional deep-layer cells in *Satb2* mutants, suggesting that mutant neurons acquire characteristics of CSMN neurons.

(G and H) Neurons that would normally express *Satb2* (as revealed by β-galactosidase staining, red) ectopically express Ctip2 (green) in the *Satb2* null cortex. Scale bar, 50 μm for panels (A)–(H).

(I–L) High-magnification images of neurons that were pulse-labeled with BrdU at E15.5 then stained for Ctip2 at E18.5, showing that cells destined to become layer 2/3 neurons ectopically express Ctip2 in *Satb2* mutants.

(I and J) In wild-type controls, BrdU^{+} cells did not express Ctip2, but numerous colabeled cells were observed in *Satb2* mutants (arrows).

(M and N) Few BrdU^{+} cells were observed in layer 5 of wild-type brains. In *Satb2* mutants, many neurons normally destined for layer 2/3 were either still migrating or abnormally stalled in layer 5; many of these cells ectopically expressed Ctip2.

(K, L, O, and P) In sections from *Satb2* mutants (J and N), immunofluorescent images for Ctip2 (red) (K and O) and BrdU (green) (L and P) are also shown separately, and double-positive cells are indicated by white arrows.

(Figures S6A and S6A′). This temporospatial window of coexpression coincides with early stages of layer 5 neuron differentiation and may reflect a brief period during which subpopulations of layer 5 neurons acquire their final fates.

To ascertain whether Satb2 is sufficient to suppress *Ctip2* expression, we electroporated *Satb2* into neural stem cells (NSCs), which were subsequently allowed to differentiate and were stained for Satb2 and Ctip2 (Figures 7A and 7B). When proliferating NSCs were electroporated with a control *gfp*$^{+}$ cDNA expression construct, ~60% and 40% of GFP^{+} neurons derived from E12.5 and E14.5 NSCs, respectively, expressed Ctip2 (Figures 7C and 7E). In contrast, electroporation with a construct containing both *myc*-tagged *Satb2* cDNA and *gfp* reporter resulted in significantly fewer (<20%) GFP^{+} neurons (Figure 7D; cytoplasmic, green) that expressed Ctip2^{+} (Figures 7D and 7E), demonstrating that Satb2 antagonizes *Ctip2* expression in neurons derived from fetal cortical NSCs.

To examine whether Satb2 regulates the expression of *Ctip2* by direct DNA binding, we searched in silico for putative MAR sequences in the *Ctip2* gene locus using the MAR-Wiz algorithm (Namciu et al., 2004). Six putative MAR sequences were identified in the 90 kb *Ctip2* locus (Figure 8A). Electrophoretic mobility shift assays (EMSA) using recombinant Satb2 protein and several radiolabeled oligonucleotides from each MAR confirmed the presence of seven bona fide Satb2-binding sites in MARs of the *Ctip2* locus. The specificity of binding was confirmed by the competition of binding with excess unlabeled oligonucleotide containing a high-affinity consensus Satb2-binding site (Figure 8B; data not shown). No competition of binding was observed upon addition of an unrelated control oligonucleotide. These data suggest that Satb2 can interact directly with multiple sequences in the *Ctip2* locus.

To determine whether any of these Satb2-binding sites are occupied by Satb2 in vivo, we performed chromatin immunoprecipitation (ChIP) with E14.5 NSCs transduced with a retrovirus encoding HA-tagged Satb2. (Antibodies capable of immunoprecipitating Satb2 are not yet available.) ChIP analysis with an anti-HA antibody and multiple primer pairs that allow for the amplification of the putative Satb2-binding sites in the *Ctip2* locus revealed a marked enrichment of five Satb2-binding sites (Figure 8C, amplicons 5′MAR, A2, A3, A4, and A5). These data suggest that repression of *Ctip2* expression by Satb2 is mediated by direct DNA binding of Satb2 to multiple MAR sequences.

Satb transcription factors can regulate gene expression by acting locally to activate or repress transcription and by altering chromatin structure at a more global level (Cai et al., 2003, 2006; Dobreva et al., 2006). To assess the role of Satb2 in transcription of *Ctip2*, we performed transient transfection assays with a Satb2 expression plasmid and a *fos-luciferase* reporter containing MAR regions A2–A4. Expression of Satb2 in transfected

Table 1. Alterations in the Expression of Cortical Cell-Type- and Layer-Specific Markers in E18.5 *Satb2* Mutant Cortex as Determined by In Situ Hybridization

Gene	Class	Pattern in *Satb2*$^{-/-}$
Cdh10	CPN general identity	severely reduced throughout CP
Dkk3	CPN general identity	lost in superficial CP and 5
Ptn	CPN early development	severely reduced throughout CP
Lmo4	CPN intermediate development	reduced in 5 and 6 mediodorsally, elevated in IZ
Cutl1/Cux1	layer 2/3 and 4 marker	lost in superficial CP
Cutl2/Cux2	layer 2/3 and 4 marker	elevated in IZ
PCDH8	layer 2/3 and 5 marker	elevated in superficial CP and 5, elevated in IZ
RORβ	layer 4 marker	lost in 4
Bcl6	strong superficial cp marker at E18	lost throughout CP
PTP4a1	strong superficial cp marker at E18	lost in superficial CP
Cdh13	CSMN general identity	elevated in superficial CP and 5
Clim1/Ldb2	CSMN early development	elevated in superficial CP and 5, reduced in 6
Ctip2	CSMN early development	elevated in superficial CP and 5
Grb14	CSMN early development	elevated in superficial CP and 5
Kitl	layer 5 and 6 marker at E18.5	elevated in superficial CP and 5
Lix1	corticotectal late development	elevated in superficial CP and 5

See Figure S4 for images of all of the genes listed. See Table S2 for a complete list of markers assayed and references. CPN, callosal projection neuron; CSMN, corticospinal motor neuron; CP, cortical plate; IZ, intermediate zone.

EL4 T cells reduced the activity of the A4-*fos-luciferase* reporter ~2-fold, whereas no change in the basal activity of the fos promoter was detected (Figure 8D). A similar repression of reporter activity was observed with the A3 element, but not with A2 and A5 (data not shown). Repression of reporter gene activity was also observed in transfected 293 cells (data not shown). Thus, Satb2 can directly repress the function of regulatory elements in the *Ctip2* locus.

To determine whether Satb2 alters chromatin structure near its binding sites in the *Ctip2* locus, we performed ChIP assays to detect histone modifications indicative of transcriptionally poised or active chromatin. In differentiated wild-type NSCs, ChIP analysis with anti-dimethyl K4 antibody detected only minor K4 dimethylation of histone H3, a mark for transcriptionally competent chromatin (Figure 8E). Similarly, ChIP experiments using an antibody against acetylated H3 showed low levels of acetylation, indicative of minimal transcriptional activity (Figure 8F). In contrast, in differentiated Satb2-deficient NSCs, significant K4 dimethylation was observed at site A4, and moderate levels of modifications were observed at amplicons A2, A3, and A5 (Figure 8E), suggesting that chromatin at these sites is transcriptionally competent or active. H3 acetylation was also observed at amplicon A5 (Figure 8F), suggesting that this site contains the most pronounced alteration of chromatin structure.

To determine whether ectopically expressed *Satb2* affects chromatin structure at the *Ctip2* locus, we used ChIP to assay histone modifications in proliferating NSCs transduced with either control or Satb2-expressing retrovirus. Since proliferating NSCs do not express endogenous *Satb2*, any repressive chromatin modifications should be due to the ectopic expression of *Satb2*. *Satb2*-transduced cells showed a marked decrease in K4 dimethylation of histone H3 at amplicons A2–A5 compared to control cells (Figure 8G). No significant differences were observed at amplicons A1, A6, or at the 5′MAR located upstream of the *Ctip2* coding region (Figure 8G). A ChIP assay with antibody against acetylated H3 indicated that amplicon A3 was significantly less acetylated in Satb2-expressing versus control NSCs; the differences were less pronounced at amplicons A4, A5, and A6 (Figure 8H). Together, these results suggest that Satb2 induces changes in histone modifications that reflect an inactive transcriptional state at the *Ctip2* locus.

DISCUSSION

Although progress has been made in elucidating the molecular mechanisms that specify subcortical projection neurons in the developing neocortex, little is known about the mechanisms that determine the fates of corticocortical projection neurons. Previous studies demonstrated that *Satb2*, which encodes a DNA-binding protein involved in chromatin regulation, is expressed by neurons of cortical layers 2 through 4 and a subset of cells in layer 5 (Britanova et al., 2005; Szemes et al., 2006). Here we show that *Satb2* is required for the normal elaboration of corticocortical connectivity. In the absence of *Satb2*, neurons that normally project axons across the corpus callosum instead extend axons toward subcortical targets. The expression of many genes is altered in the *Satb2*-deficient cortex, including that of *Ctip2*, which is both necessary and sufficient for the development of CSMNs (Arlotta et al., 2005; B. Chen and S.K.M., unpublished data). *Ctip2* expression is normally confined to the deep layers in cortex, but *Satb2* mutants show an upregulation of *Ctip2* throughout the cortex, including layers 2 through 4. Conversely, ectopic expression of *Satb2* in NSCs was sufficient to reduce the number of neurons that express *Ctip2*, suggesting that Satb2 antagonizes *Ctip2* expression. Indeed, Satb2 binds directly to MAR sequences in the *Ctip2* locus, where it modifies the structure of histones. These studies suggest that Satb2 normally represses *Ctip2* expression in callosal projection neurons.

Altered Neuronal Migration in *Satb2* Mutant Mice

The cortices of E18.5 *Satb2* mutant mice were thinner than in wild-type controls. One factor that contributed to cortical thinning is that some neurons in *Satb2* mutants exhibited a delayed migration into the CP. Migration defects were most evident for

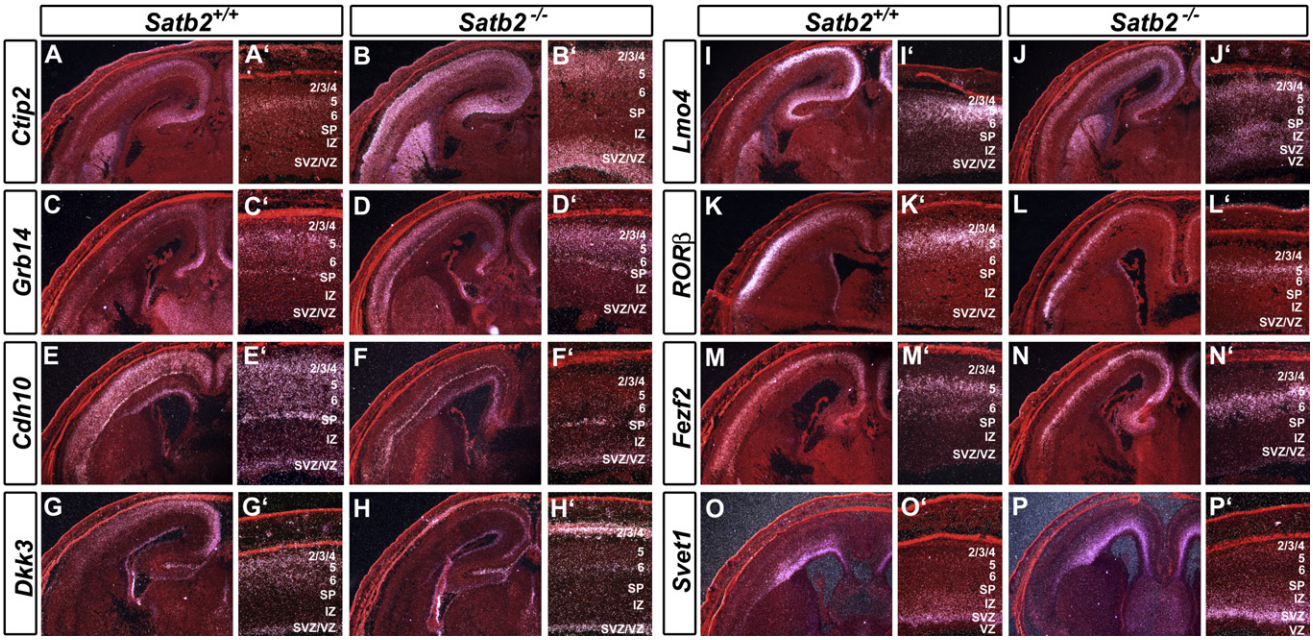

Figure 6. The Cortical Expression of CSMN and Callosal Projection Neuron Markers Is Altered in the Absence of *Satb2*

(A–D) In situ hybridization reveals that expression of the CSMN-specific genes *Ctip2* (A and B) and *Grb14* (C and D) is elevated in neurons of layers 2 through 5 neurons.

(E–J) Expression of callosal projection neuron-specific genes is either lost ([E and F], *Cdh10*; [G and H], *Dkk3*) or reduced ([I and J], *Lmo4*) in superficial CP and layer 5 neurons in the *Satb2* null cortex.

(K and L) Expression of *RORβ*, which is normally expressed in layer 4 neurons and in a subset of layer 5 neurons (K), is lost in layer 4 in *Satb2* mutants (L).

(M–P) Two examples of genes with expression patterns that do not change in *Satb2* mutants are the CSMN-specific gene *Fezf2* (M and N) and the SVZ-specific gene *Svet1* (O and P).

layer 2/3 neurons born on or after E15.5, times when endogenous *Satb2* expression in the intermediate zone is high (Britanova et al., 2005). However, not all neurons whose migration was disrupted in *Satb2* mutants transcribe the *Satb2* locus, since some $BrdU^+$ cells that showed arrested migration in the IZ were β-galactosidase$^-$. This suggests that the migration of some neurons was altered in a cell-nonautonomous manner. Defects in migration by one population of neurons can affect that of another, as was observed following electroporation of shRNAs targeting *Doublecortin* (*Dcx*) into the developing cortex. The migration of neurons in which Dcx levels were knocked down by RNAi was defective, but so too was the migration of surrounding wild-type cells (Bai et al., 2003). This is consistent with the view that neuronal migration is highly cooperative, with defects in cell movement disrupting the migration of later-generated cells. The role of *Satb2* in migrating neurons remains unclear. While it seems plausible that *Ctip2* expression by upper-layer neurons might be incompatible with normal migration, electroporation of *Ctip2* into premigratory layer 2/3 neurons results in normal migration and layer formation, even though axons are redirected subcortically (B. Chen and S.K.M., unpublished data). Our data suggest that, in addition to acquiring *Ctip2* expression, *Satb2*-deficient neurons experience broad changes in gene expression. It is plausible that conflicting gene profiles lead cells to become confused and terminate their migration prematurely.

Regulation of Callosal versus Subcortical Axonal Projections by *Satb2*

Cortical projection neurons can be classified broadly as either corticocortical neurons, which extend axons within the telencephalon to ipsilateral or contralateral targets, or subcortical projection neurons, whose targets include the thalamus, midbrain, hindbrain, and spinal cord (McConnell, 1995; Molyneaux et al., 2007). Subcortical projection neurons predominate in the early-generated layers 5 and 6, whereas corticocortical neurons are abundant in the later-generated layers 2 through 4. These two classes can also coexist within a layer (e.g., layer 5: Koester and O'Leary, 1993), raising questions about how their axon trajectories are determined during development. Our data suggest that *Satb2* plays an essential role in corticocortical neuron development.

The inclusion of a *LacZ* marker in the *Satb2* locus enabled us to identify the axons of *Satb2*-expressing neurons. Visualization of β-galactosidase in $Satb2^{+/-}$ brains revealed that the axons of *Satb2*-expressing neurons traverse the corpus callosum. These cells likely also form ipsilateral cortical connections, since previous studies using retrograde tracers (Mitchell and Macklis, 2005), reconstructions of individual callosal axons (Veinante and Deschenes, 2003), or electroporation with *channelrhodopsin-2* to examine functional connections (Petreanu et al., 2007) reveal that many callosally projecting neurons form ipsilateral as well as contralateral connections.

Table 2. Alterations in the Expression of Genes Encoding Axon Guidance Ligands and Receptors in the E18.5 *Satb2* Mutant Cortex as Determined by In Situ Hybridization

Gene	Class	Pattern in *Satb2*$^{-/-}$
EphA5	receptor, mediates *Efna* repulsion	elevated in superficial CP and 5, reduced in 6 and SP
EphA7	receptor, mediates *Efna* repulsion	elevated in superficial CP and 5
EphB1	receptor, mediates *Efnb* repulsion	elevated in superficial CP and 5
Efnb2	chemorepellant, membrane-bound	elevated in superficial CP and 5
Slit3	chemorepellant, diffusible	elevated in superficial CP and 5
Nrp1	receptor, mediates *Sema* repulsion and adhesion	elevated in superficial CP
EphB6	receptor, mediates *Efnb* repulsion	elevated in IZ, reduced in SP
Sema6D	chemorepellant, also mediates adhesion, membrane-bound	elevated in IZ
Sema3C	chemorepellant, also mediates adhesion, membrane-bound	severely reduced in 5
EphA4	receptor, mediates *Efna* repulsion	reduced throughout CP (weak 6 remains)
PlxnA4	receptor, mediates *Sema* repulsion and adhesion	reduced throughout CP
Unc5h3	receptor, mediates *Ntn* repulsion	reduced throughout CP (SP remains)

See Figure S5 for images of all of the genes listed. See Table S3 for a complete list of axon guidance molecules assayed and references. CP, cortical plate; IZ, intermediate zone; SP, subplate.

Satb2-deficient neurons showed profound alterations in their axonal projections: instead of projecting across the corpus callosum, the axons of *LacZ*$^{+}$ mutant neurons extended through the internal capsule toward subcortical targets. This novel trajectory did not reflect the simple inability of axons to cross the corpus callosum, which might arise from defects in constructing this commissure (seen commonly in mutant mice: Richards et al., 2004). A small population of L1^{+} or TAG-1^{+} axons do indeed cross the corpus callosum, and the glial wedge and glial sling, midline structures required for callosal development (Silver et al., 1982; Ashwell and Mai, 1997; Shu et al., 2003), are present in *Satb2* mutants. The expression of axon guidance molecules at the dorsal telencephalic midline appeared normal, and we did not observe Probst bundles, which are typical of mutations that disrupt callosal development (Stefanko, 1980; Ozaki and Wahlsten, 1993). Collectively, these observations suggest that the altered trajectories of β-galactosidase^{+} axons in *Satb2* mutants arise from cell-intrinsic changes in axon targeting.

We were unable to ascertain if *LacZ*$^{+}$ axons successfully innervated subcortical targets in *Satb2* mutants. β-galactosidase could be traced within the corticospinal tract into the ventral midbrain, but the axons were not visible within the spinal cord itself. It is possible that the apparent absence of axons in the spinal cord arose from technical difficulties in detecting small amounts of β-galactosidase or a failure of axons to transport β-galactosidase over long distances. Alternatively, it is possible that the axons of *LacZ*$^{+}$ neurons fail to reach the spinal cord, either because axon targeting has not been completely respecified or because their axons take longer to reach the spinal cord than do the axons of earlier-generated layer 5 neurons. It is difficult to definitively test these possibilities because *Satb2*$^{-/-}$ mice die at birth, when the axons of normal layer 5 neurons are just reaching the

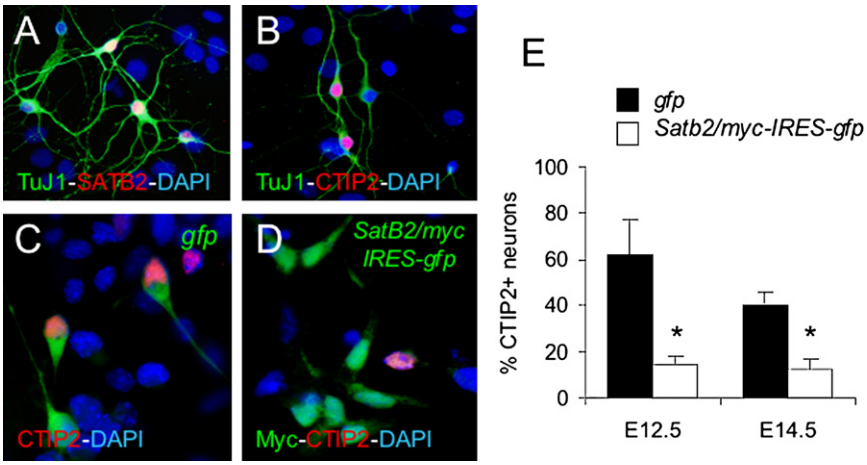

Figure 7. Overexpression of *Satb2* Represses *Ctip2* Expression in Neural Stem Cells In Vitro

(A and B) Expression of Satb2 or Ctip2 (red) and TuJ1 (green) in differentiating cultures of E14.5 cortical NSCs after 7 days in vitro. Cell counts based on these and similar images demonstrate that ~30% of TuJ1^{+} neurons express Satb2 (A) and ~60% of TuJ1^{+} neurons express Ctip2 (B).

(C and D) Differentiated cultures from E14.5 NSCs transfected with *pcDNA3.1-gfp* or with *pcDNA3.1-Satb2-myc-IRES-gfp*. (C) Control cultures transfected with *gfp* vector contained many cells that expressed Ctip2 (red). (D) Fewer Ctip2^{+} cells (red) were observed in cultures transfected with *Satb2-myc-ires-gfp* as visualized by GFP fluorescence (cytoplasmic labeling, green), Ctip2 (red), and myc (nuclear, green) immunostaining.

(E) Quantitation of the percentages of Ctip2^{+} neurons in cultures from E12.5 and E14.5 fetal cortical NSCs transfected with *pcDNA3.1-gfp* or with *pcDNA3.1-Satb2-myc-IRES-gfp.* The proportion of Ctip2^{+} neurons in the *Satb2*-transduced population was significantly reduced. Student's t test (after arcsen transformation of relative values): *$p < 0.05$, $n = 3$ in each case. Error bars show mean ± SD.

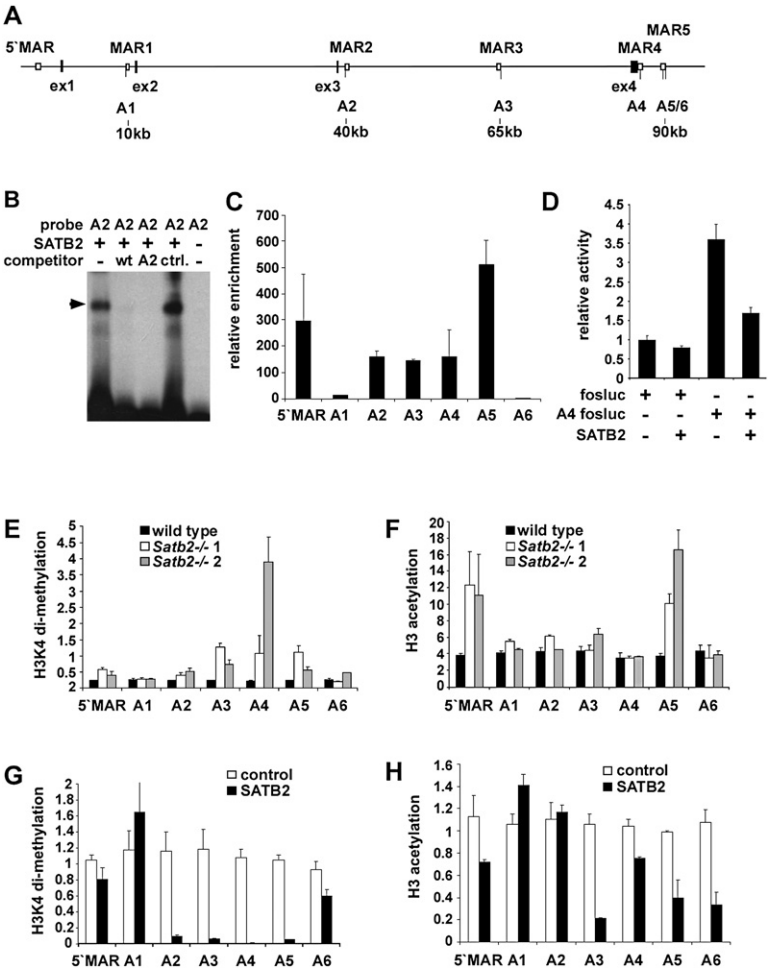

Figure 8. Satb2 Binds to MAR Sequences from Regulatory Sequences in the *Ctip2* Locus, Suggesting that Satb2 Represses *Ctip2* Expression Directly

(A) Schematic representation of the *Ctip2* locus. Black bars indicate exons 1–4 (ex1–ex4). Matrix attachment regions 1–6 (5′MAR and MAR1–5) are shown as open bars. ChIP amplicons 1–6 (A1–A6) and their position in the locus are depicted below. Basepair count begins at ATG of exon 1.

(B) Electrophoretic mobility shift assay (EMSA) showing binding of purified recombinant Satb2 to A2 EMSA probe. A wild-type MAR probe (wt), A2 probe, and a negative control (ctrl.) were added as competitor in 250-fold molar excess.

(C) ChIP assay to detect Satb2 occupancy at the *Ctip2* locus in NSCs. Error bars represent the standard deviation of two experiments.

(D) A4 sequence activity in presence or absence of Satb2 in EL4 cells transfected with a *fos-luciferase* reporter construct that either contained or lacked the A4 sequence.

(E and F) ChIP assay to detect changes in H3 K4 dimethylation (E) and H3 acetylation (F) at the *Ctip2* locus in differentiated wild-type and *Satb2*$^{-/-}$ NSCs. Error bars represent the standard deviation of two experiments.

(G and H) ChIP assay to detect changes in H3 K4 dimethylation (G) and H3 acetylation (H) at the *Ctip2* locus in proliferating wild-type NSCs with and without overexpression of *Satb2*. Error bars represent the standard deviation of two experiments.

spinal cord (O'Leary and Koester, 1993; Kasper et al., 1994; Molnar and Cheung, 2006). Nevertheless, the presence of β-galactosidase^{+} axons in the corticospinal tract provides strong evidence for the respecification of callosal projection neuron identity in the absence of *Satb2*.

Satb2 Represses *Ctip2* Expression in Corticocortical Projection Neurons

The molecular basis of this fate change is likely due, at least in part, to the derepression of *Ctip2* in the *Satb2* mutant cortex. *Ctip2* is necessary and sufficient for the development of CSMNs: deletion of *Ctip2* results in a failure of CSMN axons to reach the spinal cord (Molyneaux et al., 2005), and overexpression of *Ctip2* in layer 2/3 neurons redirects their axons toward the spinal cord (B. Chen and S.K.M., unpublished data). Using immunohistochemistry and in situ hybridization, we observed increased numbers of Ctip2^{+} neurons in layers 2 through 5 of *Satb2* mutant brains, suggesting that the *Satb2* knockout phenocopies the overexpression of *Ctip2*.

Ctip2 is one of several genes implicated in the specification of subcortical projection neurons in developing cortex. *Fezf2* is also both necessary and sufficient for CSMN development and is required for *Ctip2* expression in layer 5 subcortical projection neurons (Chen et al., 2005a, 2005b; Molyneaux et al., 2005; B. Chen and S.K.M., unpublished data). Interestingly, the *Fezf2* expression domain was not expanded in *Satb2* mutants, nor did we observe expanded expression of *ER81*, *FoxO1*, or *Crystallin mu*, CSMN-specific genes that are misregulated in *Fezf2* mutants (Chen et al., 2005a). These data suggest that *Satb2*$^{-/-}$ neurons may not have adopted all characteristics of normal subcortical projection neurons by E18.5. On the other hand, some of these genes (e.g., *ER81*: Hevner et al., 2003; Molnar and Cheung, 2006; Yoneshima et al., 2006) are not required for normal CSMN development, whereas others (e.g., *Fezf2*) affect axon projections by regulating the expression of key effectors. In the absence of *Fezf2*, layer 5 CSMNs form cortical connections; however, overexpression of *Ctip2* in *Fezf2*-deficient layer 5 neurons rescues mutant neurons and enables them to extend subcortical axons (B. Chen and S.K.M., unpublished data). These studies suggest that *Ctip2* is a key determinant of CSMN fate and are consistent with the notion that *Satb2*-deficient neurons overexpress *Ctip2* and thus become bona fide subcortical projection neurons, even in the absence of *Fezf2* expression.

Satb2 Binds to and Represses the Expression of *Ctip2*

Satb2 appears to directly repress *Ctip2* expression in developing cortical neurons. Ctip2 expression expands in *Satb2* mutants, and overexpression of *Satb2* in NSCs markedly decreases the number of Ctip2^{+} neurons that differentiate in vitro. When we electroporated expression constructs encoding *Satb2* and *gfp* into the precursors of deep-layer neurons at E12.5 in vivo, we observed no obvious reduction in Ctip2

expression in *Satb2*-electroporated cells (E.A.A., unpublished data). Interestingly, wild-type cortical neurons can coexpress Satb2 and Ctip2 during layer 5 formation (Figure S6), when *Satb2* expression levels are relatively low (Figure 1B). We do not know whether we failed to produce high enough levels of Satb2 to repress *Ctip2*, or whether *Ctip2* regulation in vivo is complicated, for example, by signaling events that locally reinforce cell-fate decisions.

Previous studies have shown that Satb2 and its homolog Satb1 affect transcription by binding to and mediating the anchoring of DNA MARs to the nuclear matrix, thus altering chromatin structure and the accessibility of genes to transcriptional machinery (Yasui et al., 2002; Cai et al., 2003, 2006; Dobreva et al., 2003). The *Ctip2* genomic locus contains multiple MARs upstream and downstream of the *Ctip2* open reading frame, and EMSA results indicate that these elements interact physically with Satb2. Our ChIP experiments revealed that Satb2 binds to multiple MAR sites in vivo and that Satb2 induces changes in chromatin structure, as reflected by the K4 dimethylation and acetylation of histone H3. Dimethylation of K4 of histone H3 and H3 acetylation correlate globally with an "open" chromatin structure (Encode, 2007), and, consistent with the Satb2-mediated repression of *Ctip2*, Satb2-deficient differentiated NSCs display an increase in K4 dimethylation and acetylation of histone H3 in the vicinity of the Satb2 binding sites A3, A4, and A5. Conversely, we detected marked decreases in H3K4 dimethylation in proliferating NSCs transduced with a Satb2-expressing retrovirus. These observations suggest that Satb2 binds to multiple regulatory elements of the *Ctip2* open reading frame to generate a heterochromatic environment that prevents *Ctip2* expression.

In support of this notion, Satb2 represses *Hoxa2* expression by binding to a MAR element in differentiating osteoblasts (Dobreva et al., 2006). Satb1, a close relative of Satb2, can recruit histone deacetylases to promoters (Pavan Kumar et al., 2006). Interestingly, Ctip2 exerts its effects on target gene expression by generating a heterochromatin environment that inhibits transcription (Marban et al., 2007). It remains to be seen if ectopically expressed *Ctip2* reprograms layer 2/3 neurons to become subcortical projection neurons by inhibiting *Satb2* expression and if such inhibition is exerted via chromatin remodeling. Our observation of Ctip2$^+$/β-galactosidase$^+$ neurons in *Satb2* mutant brains (Figure 5H) suggests that Ctip2 alone cannot inhibit expression from the *Satb2* promoter.

Although our data implicate Satb2 as a major regulator of *Ctip2* expression, other factors likely regulate *Ctip2* expression as well. Our luciferase reporter studies reveal that factors expressed in EL4 cells can activate transcription from the A4 amplicon of the *Ctip2* locus, and in silico analyses of MAR sites A4 and A5 in the *Ctip2* locus reveal binding sites for a number of transcription factors (data not shown). It remains to be seen whether these transcription factors actually regulate *Ctip2* expression in developing neurons and if that regulation is synergistic with, antagonistic to, or independent of Satb2 activity.

Satb2 Regulates the Expression of Numerous Genes in the Developing Cortex

Chromatin remodeling is an effective mechanism by which transcription factors exert long-range effects on many genes, bestowing such factors with the potential to be "master regulators" of cell-fate specification. Targeted inactivation of *Satb2* results in the misregulation of 27 of 93 genes we assayed by in situ hybridization. Genes exhibiting expanded expression included CSMN-specific genes, layer 5-specific genes, and axon guidance receptors that had not previously been implicated in pathfinding to subcortical targets. In addition, we observed reductions or losses in the expression of genes normally expressed in corticocortical projection neurons, and of three axon guidance receptors not previously implicated in pathfinding to corticocortical or callosal targets. While the transcription of some of these genes may have been altered because of ectopic *Ctip2* expression in *Satb2*-deficient neurons, it is also possible that Satb2 directly regulates their transcription. Although much remains to be learned about the role of Satb2 in specifying the fates of corticocortical projection neurons, it seems likely that Satb2-directed chromatin remodeling inhibits the CSMN fate and promotes the specification of corticocortical neuronal identity, suggesting that Satb2 is an essential regulator of axonal connectivity in the developing neocortex.

EXPERIMENTAL PROCEDURES

Animals

Satb2 mutant mice were generated and genotyped as described previously (Dobreva et al., 2006), with the morning of vaginal plug observation considered as E0.5.

Histology, Immunohistochemistry, and In Situ Hybridization

BrdU was injected into pregnant females at 50 mg/kg body weight. Standard methods for fixation and immunohistochemistry were used; see Supplemental Data for details. In situ hybridization was performed as described previously (Frantz et al., 1994); see Table S1 for a complete list of probes.

Neural Stem Cell Culture

NSC cultures were prepared essentially as described (Reynolds et al., 1992; Parmar et al., 2002; Ferron et al., 2007); see Supplemental Data for details. NSCs were transduced using Nucleofector (II) program A-33 (Amaxa Biosystems) and Mouse NSC Nucleofector Kit VPG-1004 (Amaxa Biosystems) with *pcDNA3.1-Satb2-myc-IRES-gfp* (3 μg), *pcDNA3.1-gfp* (3 μg), and *pmaxGFP*™ (1 μg, as a positive control of nucleofection) plasmids. For differentiation assays, neurospheres were dissociated and cells plated onto Matrigel-coated plates without mitogens. Cells were fixed in 4% PFA for 20 min after 2 or 7 days in vitro. See Supplemental Data for details on immunostaining.

Electrophoretic Mobility Shift Assay

His-tagged Satb2 for EMSA was expressed and purified as described previously (Dobreva et al,. 2003). Oligonucleotides for use in EMSA were chosen after analyzing potential MAR sequences using Genomatix software. Oligonucleotides were radiolabeled with ^{32}P and purified on a 20% native polyacrylamide gel. DNA binding reactions contained 10 mM HEPES, pH 7.9, 50 mM KCl, 2.5 mM $MgCl_2$, 0.5 mM EDTA, 1 mM DTT, 300 μg/ml BSA, 8% glycerol, 0.5 μg poly dI-dC, and 10,000 cpm radiolabeled probe. EMSAs were performed in 0.33× TBE. Sequences of oligonucleotides used for EMSA are presented in Supplemental Data.

Chromatin Immunoprecipitation Assay

cDNA encoding HA-tagged-Satb2 was cloned into the retroviral vector pEGZ/MCS. Phoenix cells transfected with *pEGZ/MCS-HA-Satb2-IRES-gfp* and *pEGZ-MCS-gfp* plasmids were grown in NSC growth medium, and medium containing retrovirus was collected 24 hr later. Cortical NSCs dissociated from E14.5 embryos were plated at high density (1 × 10^5 cells/ml) in NSC growth medium. After 48 hr in vitro, cells were collected and resuspended in

medium containing virus supplemented with 8 μg/ml polybrene. After 8 hr in vitro, neurospheres were replated in fresh growth medium for 12 hr, and the infection procedure was repeated. GFP expression was detected by fluorescence microscopy and cytometry, and cells were sorted by FACS for ChIP analysis. Crosslinking of proteins and sonication of DNA were performed as described (Dobreva et al., 2006).

Immunoprecipitation with 2 μg anti-HA mAb were carried out overnight at 4°C. Immune complex was collected with salmon-sperm-saturated protein G for 30 min and washed three times with high-salt buffer (20 mM Tris at pH 8.0, 0.1% SDS, 1% NP-40, 2 mM EDTA, and 0.5 M NaCl) followed by three washes in no-salt buffer (1 × TE). Immune complexes were extracted in 1 TE containing 2% SDS and protein; DNA crosslinks were reverted by heating at 65°C overnight. After proteinase K digestion (100 μg for 2 hr), DNA was extracted with phenol-chloroform and precipitated in ethanol. About 1/20 of the immunoprecipitated DNA was used in each PCR. See Supplemental Data for primers used for RT-PCR.

Luciferase Assay

EL4 cells were electroporated with p*fos*luc or a p*fos*luc vector containing amplicons of A2–A5 and were cotransfected with or without 0.3 μg Satb2. Cells were harvested after 30 hr. The luciferase assay system (Promega Cat. #1501) was used per manufacturer's instructions. See Supplemental Data for primer sequences for luciferase constructs.

Promoter Analysis for Transcription Factor Binding Sites

The human and mouse promoter and regulatory sequences upstream and downstream of the *Ctip2* coding sequence were assayed in silico by Genomatix software to identify potential transcription factor binding sites. The resulting lists were cross-referenced against regions of 100% homology between the mouse and human sequences to identify transcription factor binding sites in the *Ctip2* locus that were 100% conserved between human and mouse.

Supplemental Data

The Supplemental Data for this article can be found online at http://www.neuron.org/cgi/content/full/57/3/364/DC1/.

ACKNOWLEDGMENTS

We thank C. Kaznowski, S. Martin, S. Srinivasan, I. Falk, C. Giachino, and C. Andreu for assistance with critical experiments; A. Candia for help with figures and tables; S. Wang, A. O'Reilly, and A. Candia for scientific discussions; R. Hevner for Tbr1 antibody; O. Cases for Cux2 antibody; F. Savarese for the HA-*Satb2* construct; and B. Chen, A. Okada, J. Hébert, R. Friedel, J. Rong, and L. Ma for in situ hybridization probes. Funded by NIH EY08411 to S.K.M., funds of the Max-Planck Society to R.G., and grants from the Ministerio de Educación y Ciencia (SAF2005-06325), Ministerio de Sanidad (TerCel and CIBERNED), and Fundación la Caixa to I.F.

Received: June 9, 2007
Revised: October 23, 2007
Accepted: December 3, 2007
Published: February 6, 2008

REFERENCES

Arlotta, P., Molyneaux, B.J., Chen, J., Inoue, J., Kominami, R., and Macklis, J.D. (2005). Neuronal subtype-specific genes that control corticospinal motor neuron development in vivo. Neuron *45*, 207–221.

Ashwell, K.W., and Mai, J.K. (1997). A transient CD15 immunoreactive sling in the developing mouse cerebellum. Int. J. Dev. Neurosci. *15*, 883–889.

Auladell, C., Martinez, A., Alcantara, S., Super, H., and Soriano, E. (1995). Migrating neurons in the developing cerebral cortex of the mouse send callosal axons. Neuroscience *64*, 1091–1103.

Bagri, A., Marin, O., Plump, A.S., Mak, J., Pleasure, S.J., Rubenstein, J.L., and Tessier-Lavigne, M. (2002). Slit proteins prevent midline crossing and determine the dorsoventral position of major axonal pathways in the mammalian forebrain. Neuron *33*, 233–248.

Bai, J., Ramos, R.L., Ackman, J.B., Thomas, A.M., Lee, R.V., and LoTurco, J.J. (2003). RNAi reveals doublecortin is required for radial migration in rat neocortex. Nat. Neurosci. *6*, 1277–1283.

Barallobre, M.J., Del Rio, J.A., Alcantara, S., Borrell, V., Aguado, F., Ruiz, M., Carmona, M.A., Martin, M., Fabre, M., Yuste, R., et al. (2000). Aberrant development of hippocampal circuits and altered neural activity in netrin 1-deficient mice. Development *127*, 4797–4810.

Britanova, O., Akopov, S., Lukyanov, S., Gruss, P., and Tarabykin, V. (2005). Novel transcription factor Satb2 interacts with matrix attachment region DNA elements in a tissue-specific manner and demonstrates cell-type-dependent expression in the developing mouse CNS. Eur. J. Neurosci. *21*, 658–668.

Brown, L.L., Smith, D.M., and Goldbloom, L.M. (1998). Organizing principles of cortical integration in the rat neostriatum: corticostriate map of the body surface is an ordered lattice of curved laminae and radial points. J. Comp. Neurol. *392*, 468–488.

Cai, S., Han, H.J., and Kohwi-Shigematsu, T. (2003). Tissue-specific nuclear architecture and gene expression regulated by SATB1. Nat. Genet. *34*, 42–51.

Cai, S., Lee, C.C., and Kohwi-Shigematsu, T. (2006). SATB1 packages densely looped, transcriptionally active chromatin for coordinated expression of cytokine genes. Nat. Genet. *38*, 1278–1288.

Canty, A.J., Greferath, U., Turnley, A.M., and Murphy, M. (2006). Eph tyrosine kinase receptor EphA4 is required for the topographic mapping of the corticospinal tract. Proc. Natl. Acad. Sci. USA *103*, 15629–15634.

Chen, B., Schaevitz, L.R., and McConnell, S.K. (2005a). Fezl regulates the differentiation and axon targeting of layer 5 subcortical projection neurons in cerebral cortex. Proc. Natl. Acad. Sci. USA *102*, 17184–17189.

Chen, J.G., Rasin, M.R., Kwan, K.Y., and Sestan, N. (2005b). Zfp312 is required for subcortical axonal projections and dendritic morphology of deep-layer pyramidal neurons of the cerebral cortex. Proc. Natl. Acad. Sci. USA *102*, 17792–17797.

Dobreva, G., Chahrour, M., Dautzenberg, M., Chirivella, L., Kanzler, B., Farinas, I., Karsenty, G., and Grosschedl, R. (2006). SATB2 is a multifunctional determinant of craniofacial patterning and osteoblast differentiation. Cell *125*, 971–986.

Dobreva, G., Dambacher, J., and Grosschedl, R. (2003). SUMO modification of a novel MAR-binding protein, SATB2, modulates immunoglobulin mu gene expression. Genes Dev. *17*, 3048–3061.

Encode (2007). Identification and analysis of functional elements in 1% of the humane genome by the Encode pilot project. Nature *447*, 799–816.

Ferron, S.R., Andreu-Agullo, C., Mira, H., Sanchez, P., Marques-Torrejon, M.A., and Farinas, I. (2007). A combined ex/in vivo assay to detect effects of exogenously added factors in neural stem cells. Nat. Protocols *2*, 849–859.

Finger, J.H., Bronson, R.T., Harris, B., Johnson, K., Przyborski, S.A., and Ackerman, S.L. (2002). The netrin 1 receptors Unc5h3 and Dcc are necessary at multiple choice points for the guidance of corticospinal tract axons. J. Neurosci. *22*, 10346–10356.

Frantz, G.D., Bohner, A.P., Akers, R.M., and McConnell, S.K. (1994). Regulation of the POU-domain gene SCIP during cerebral cortical development. J. Neurosci. *14*, 472–485.

Fujimori, K.E., Takeuchi, K., Yazaki, T., Uyemura, K., Nojyo, Y., and Tamamki, N. (2000). Expression of L1 and TAG-1 in the corticospinal, callosal, and hippocampal commissural neurons in the developing rat telencephalon as revealed by retrograde and in situ hybridization double labeling. J. Comp. Neurol. *417*, 275–288.

Hevner, R.F., Daza, R.A., Rubenstein, J.L., Stunnenberg, H., Olavarria, J.F., and Englund, C. (2003). Beyond laminar fate: toward a molecular classification of cortical projection/pyramidal neurons. Dev. Neurosci. *25*, 139–151.

Hevner, R.F., Miyashita-Lin, E., and Rubenstein, J.L. (2002). Cortical and thalamic axon pathfinding defects in Tbr1, Gbx2, and Pax6 mutant mice: evidence that cortical and thalamic axons interact and guide each other. J. Comp. Neurol. *447*, 8–17.

Hevner, R.F., Shi, L., Justice, N., Hsueh, Y.P., Sheng, M., Smiga, S., Bulfone, A., Goffinet, A.M., Campagnoni, A.T., and Rubenstein, J.L.R. (2001). Tbr1 regulates differentiation of the preplate and layer 6. Neuron *29*, 353–366.

Jenuwein, T., Forrester, W.C., Fernandez-Herrero, L.A., Laible, G., Dull, M., and Grosschedl, R. (1997). Extension of chromatin accessibility by nuclear matrix attachment regions. Nature *385*, 269–272.

Kasper, E.M., Lubke, J., Larkman, A.U., and Blakemore, C. (1994). Pyramidal neurons in layer 5 of the rat visual cortex. III. Differential maturation of axon targeting, dendritic morphology, and electrophysiological properties. J. Comp. Neurol. *339*, 495–518.

Koester, S.E., and O'Leary, D.D. (1993). Connectional distinction between callosal and subcortically projecting cortical neurons is determined prior to axon extension. Dev. Biol. *160*, 1–14.

Koester, S.E., and O'Leary, D.D. (1994). Development of projection neurons of the mammalian cerebral cortex. Prog. Brain Res. *102*, 207–215.

Kullander, K., Croll, S.D., Zimmer, M., Pan, L., McClain, J., Hughes, V., Zabski, S., DeChiara, T.M., Klein, R., Yancopoulos, G.D., et al. (2001a). Ephrin-B3 is the midline barrier that prevents corticospinal tract axons from recrossing, allowing for unilateral motor control. Genes Dev. *15*, 877–888.

Kullander, K., Mather, N.K., Diella, F., Dottori, M., Boyd, A.W., and Klein, R. (2001b). Kinase-dependent and kinase-independent functions of EphA4 receptors in major axon tract formation in vivo. Neuron *29*, 73–84.

Lindwall, C., Fothergill, T., and Richards, L.J. (2007). Commissure formation in the mammalian forebrain. Curr. Opin. Neurobiol. *17*, 3–14.

Marban, C., Suzanne, S., Dequiedt, F., de Walque, S., Redel, L., Van Lint, C., Aunis, D., and Rohr, O. (2007). Recruitment of chromatin-modifying enzymes by Ctip2 promotes HIV-1 transcriptional silencing. EMBO J. *26*, 412–423.

McConnell, S.K. (1995). Constructing the cerebral cortex: neurogenesis and fate determination. Neuron *15*, 761–768.

Mintz, C.D., Dickson, T.C., Gripp, M.L., Salton, S.R., and Benson, D.L. (2003). ERMs colocalize transiently with L1 during neocortical axon outgrowth. J. Comp. Neurol. *464*, 438–448.

Mitchell, B.D., and Macklis, J.D. (2005). Large-scale maintenance of dual projections by callosal and frontal cortical projection neurons in adult mice. J. Comp. Neurol. *482*, 17–32.

Molnar, Z., and Cheung, A.F. (2006). Towards the classification of subpopulations of layer V pyramidal projection neurons. Neurosci. Res. *55*, 105–115.

Molyneaux, B.J., Arlotta, P., Hirata, T., Hibi, M., and Macklis, J.D. (2005). Fezl is required for the birth and specification of corticospinal motor neurons. Neuron *47*, 817–831.

Molyneaux, B.J., Arlotta, P., Menezes, J.R., and Macklis, J.D. (2007). Neuronal subtype specification in the cerebral cortex. Nat. Rev. Neurosci. *8*, 427–437.

Namciu, S.J., Friedman, R.D., Marsden, M.D., Sarausad, L.M., Jasoni, C.L., and Fournier, R.E. (2004). Sequence organization and matrix attachment regions of the human serine protease inhibitor gene cluster at 14q32.1. Mamm. Genome *15*, 162–178.

O'Leary, D.D., and Koester, S.E. (1993). Development of projection neuron types, axon pathways, and patterned connections of the mammalian cortex. Neuron *10*, 991–1006.

Ozaki, H.S., and Wahlsten, D. (1993). Cortical axon trajectories and growth cone morphologies in fetuses of acallosal mouse strains. J. Comp. Neurol. *336*, 595–604.

Ozaki, H.S., and Wahlsten, D. (1998). Timing and origin of the first cortical axons to project through the corpus callosum and the subsequent emergence of callosal projection cells in mouse. J. Comp. Neurol. *400*, 197–206.

Parmar, M., Skogh, C., Bjorklund, A., and Campbell, K. (2002). Regional specification of neurosphere cultures derived from subregions of the embryonic telencephalon. Mol. Cell. Neurosci. *21*, 645–656.

Pavan Kumar, P., Purbey, P.K., Sinha, C.K., Notani, D., Limaye, A., Jayani, R.S., and Galande, S. (2006). Phosphorylation of SATB1, a global gene regulator, acts as a molecular switch regulating its transcriptional activity in vivo. Mol. Cell *22*, 231–243.

Petreanu, L., Huber, D., Sobczyk, A., and Svoboda, K. (2007). Channelrhodopsin-2-assisted circuit mapping of long-range callosal projections. Nat. Neurosci. *10*, 663–668.

Reiner, A., Jiao, Y., Del Mar, N., Laverghetta, A.V., and Lei, W.L. (2003). Differential morphology of pyramidal tract-type and intratelencephalically projecting-type corticostriatal neurons and their intrastriatal terminals in rats. J. Comp. Neurol. *457*, 420–440.

Reynolds, B.A., Tetzlaff, W., and Weiss, S. (1992). A multipotent EGF-responsive striatal embryonic progenitor cell produces neurons and astrocytes. J. Neurosci. *12*, 4565–4574.

Richards, L.J., Plachez, C., and Ren, T. (2004). Mechanisms regulating the development of the corpus callosum and its agenesis in mouse and human. Clin. Genet. *66*, 276–289.

Rouiller, E.M., and Welker, E. (1991). Morphology of corticothalamic terminals arising from the auditory cortex of the rat: a Phaseolus vulgaris-leucoagglutinin (PHA-L) tracing study. Hear. Res. *56*, 179–190.

Shu, T., Li, Y., Keller, A., and Richards, L.J. (2003). The glial sling is a migratory population of developing neurons. Development *130*, 2929–2937.

Silver, J., Lorenz, S.E., Wahlsten, D., and Coughlin, J. (1982). Axonal guidance during development of the great cerebral commissures: descriptive and experimental studies, in vivo, on the role of preformed glial pathways. J. Comp. Neurol. *210*, 10–29.

Stefanko, S.Z. (1980). Fasciculus callosus longitudinalis (bundle of Probst) and its relation to the corpus callosum. Patol. Pol. *31*, 263–272.

Szemes, M., Gyorgy, A., Paweletz, C., Dobi, A., and Agoston, D.V. (2006). Isolation and characterization of SATB2, a novel AT-rich DNA binding protein expressed in development- and cell-specific manner in the rat brain. Neurochem. Res. *31*, 237–246.

Takeuchi, A., Hamasaki, T., Litwack, E.D., and O'Leary, D.D. (2006). Novel IgCAM, MDGA1, expressed in unique cortical area- and layer-specific patterns and transiently by distinct forebrain populations of Cajal-Retzius neurons. Cereb. Cortex *17*, 1531–1541.

Tarabykin, V., Stoykova, A., Usman, N., and Gruss, P. (2001). Cortical upper layer neurons derive from the subventricular zone as indicated by Svet1 gene expression. Development *128*, 1983–1993.

Veinante, P., and Deschenes, M. (2003). Single-cell study of motor cortex projections to the barrel field in rats. J. Comp. Neurol. *464*, 98–103.

Wilson, C.J. (1987). Morphology and synaptic connections of crossed corticostriatal neurons in the rat. J. Comp. Neurol. *263*, 567–580.

Wolfer, D.P., Henehan-Beatty, A., Stoeckli, E.T., Sonderegger, P., and Lipp, H.P. (1994). Distribution of TAG-1/axonin-1 in fibre tracts and migratory streams of the developing mouse nervous system. J. Comp. Neurol. *345*, 1–32.

Yasui, D., Miyano, M., Cai, S., Varga-Weisz, P., and Kohwi-Shigematsu, T. (2002). SATB1 targets chromatin remodelling to regulate genes over long distances. Nature *419*, 641–645.

Yoneshima, H., Yamasaki, S., Voelker, C.C., Molnar, Z., Christophe, E., Audinat, E., Takemoto, M., Nishiwaki, M., Tsuji, S., Fujita, I., et al. (2006). Er81 is expressed in a subpopulation of layer 5 neurons in rodent and primate neocortices. Neuroscience *137*, 401–412.